Quantification of the viscoelasticity of the bond of biotic and abiotic particles adhering to solid-liquid interfaces using a window-equipped quartz crystal microbalance with dissipation

Rebecca van der Westen[a], Henny C. van der Mei[a], Hans De Raedt[b], Adam L.J. Olsson[a,c], Henk J. Busscher[a], Prashant K. Sharma[a,*]

[a] University of Groningen and University, Medical Center Groningen, Department of Biomedical Engineering, P.O. Box 196, 9700 AD, Groningen, The Netherlands
[b] University of Groningen, Faculty of Mathematics and Natural Sciences, Computational Physics, Zernike Institute for Advanced Materials, Nijenborgh 4, 9747 AG Groningen, The Netherlands
[c] McGill University, Montreal, Department of Chemical Engineering, Quebec H3A 2B2, Canada

ARTICLE INFO

ABSTRACT

The quartz-crystal-microbalance-with-dissipation (QCM-D) has become a powerful tool for studying the bond viscoelasticity of biotic and abiotic colloidal particles adhering to substratum surfaces. A window-equipped QCM-D allows high-throughput analysis of the average bond viscoelasticity, measuring over 10^6 particles simultaneously in one single experiment. Other techniques require laborious analyses of individual particles. In this protocol, the quantitative derivation of the spring-constant and drag-coefficient of the bond between adhering colloidal particles and substratum surfaces using QCM-D is explained for bacteria and silica particles, using the particle-mass derived for validation. Bond viscoelasticity is calculated using a coupled resonator model, paying special attention to the protocol for mathematical fitting needed to obtain reliable quantitative output. Knowledge of the viscoelasticity of the bond between colloidal particles and substratum surfaces facilitates development of new strategies to detach adhering particles from or retain them on a surface.

© 2016 Elsevier B.V. All rights reserved.

1. Introduction

Control over the adhesion of biotic (such as bacteria) and abiotic colloidal particles (such as silica, polystyrene or latex particles) is a key concern in engineering and medicine. In particular, adhesion of bacteria to surfaces can form a hazard to human health [1], while adhesion control of abiotic particles is essential in areas such as sensing and data storage [2,3]. The bond between a colloidal particle and a substratum surface is seldom rigid and mostly comprises an elastic and viscous component [4,5]. The viscoelasticity of a bond is not only determinant for particle adhesion, but also for the mechanism of particle detachment [6,7]. For bacteria, the viscoelastic properties of their bond with a substratum surface often allow adhering bacteria to remain adhering under shear conditions through gradual elongation of the bond [8].

Several experimental techniques have been developed to study the adhesive bond between adhering colloidal particles and a substratum surface, such as the use of atomic force microscopy (AFM) [9–11] and optical or magnetic tweezers [12]. In these techniques, a single colloidal particle is forced to contact a substratum surface after which it is pulled off and the force required to break the bond is taken as the adhesive force. Elasticity and viscosity of the bond can be measured using AFM by pressing a particle on a substratum surface under a constant, applied force and measuring deformation or by measuring the force resulting from an applied, constant deformation of the particle. Using this approach, Lu et al. [13] described the bond components of bacterial cell surfaces as a spring, representing the elastic component as recognized in the standard solid model, placed in a series with a combination of a spring and a dashpot in parallel. In order to ensure that such modeling only comprises the bond between an adhering particle and a substratum surface and not the bulk of a particle as in traditional Hertz, Johnson-Kendall-Roberts or Derjaguin-Muller-Toropov models, Chen et al. [14] suggested to consider the bond between an adhering particle and a substratum surface as a cylin-

drical volume that deforms under conditions of constant volume to provide a method allowing to confine traditional analysis to the bond itself. Analysis of the Brownian motion induced nanoscopic vibrations exhibited by biotic [15] and abiotic [7,16] colloidal particles offers a completely different way to obtain the elasticity of the bond, with smaller vibrational amplitudes being indicative of higher elasticity [15]. Apart from the assumptions involved in each of the above-mentioned techniques, they all possess the common limitation that adhering particles must be studied one-by-one on an individual basis, which makes it hard to obtain statistically reliable, quantitative data.

The quartz-crystal-microbalance-with-dissipation (QCM-D) effectively avoids this "one-by-one" drawback, and has been applied to analyze the viscoelasticity of the bond between biotic and abiotic particles adhering to solid-liquid interfaces over large numbers of adhering particles, typically in the order of 10^{10} per m^2 of a sensor surface, approximately equivalent to 10^6 particles on the sensor surface. Nanometer-scale shear oscillations of the sensor cause deformation of the bonds with an adhering particle, with an opposing force arising from the surrounding liquid. The QCM-D registers the shift in resonance frequency of the sensor (Δf) due to particle adhesion as well as the energy loss to the surrounding liquid (change in "dissipation" (ΔD)). Moreover, for studies involving colloidal particles, it is advantageous to use a QCM-D equipped with a window chamber, allowing simultaneous microscopic registration of the number of particles adhering to the sensor surface.

Traditionally, QCM-D has been mostly used to determine adsorption of molecular mass to a sensor surface, assuming the adsorbed mass directly couples to the sensor surface. According to Sauerbrey's relation [17], an adsorbed coupled mass increases the effective sensor mass, yielding a reduction in the sensor resonance frequency, or in QCM-terms a negative (resonance) frequency shift. Since the penetration depth for the shear wave in QCM-D is less than 250 nm (at 5 MHz), this represents the maximum thickness of adsorbed films that can be reliably measured. The sensitivity of the mass detection in QCM is in the nanogram range. Particles however, do not necessarily mass-couple to the sensor surface, but instead may adhere as coupled resonators [18–21]. The sensor resonates at different fixed frequencies. A 5 MHz sensor resonates not only at 5 MHz but also at its overtones (15, 25 up to 65 MHz). Provided not touching each other, all colloidal particles adhering to the sensor surface act as individual, coupled resonators (Fig. 1a) with an impact on the resonance frequency shift (Δf) measured. Energy dissipation change (ΔD) is maximal when the particle resonance frequency (f_p) matches the sensor resonance frequency (f_s). The development of the coupled resonator model has greatly widened the possibilities of QCM-D, which were previously confined to molecular mass adsorption. It is interesting to note that whereas bond viscoelasticities of individual particles of the same kind often show large variations [8,15,22], QCM-D identifies a well-defined zero-value in sensor resonance frequency shift (Δf_s) when particle and sensor resonance frequencies match (zero crossing frequency (f_{ZC}), see Fig. 1b). Zero crossing frequencies are only observed when the adhering colloidal particles oscillate at frequencies within the window of the sensor resonance frequency and its observable overtones, which range from 5 MHz to 65 MHz (see Fig. 1b). Positive frequency shifts observed in the literature, could not be explained prior to the introduction of the coupled resonator model [4,5,19].

In the coupled resonator model, the frequency shifts and dissipation changes derived from the QCM-D can be related in a Kelvin-Voigt model to the viscoelasticity of the bond according to

$$\Delta f + \frac{i\Delta D f_s}{2} = \frac{f_F m_p}{\pi Z_q} \cdot N_p \left[\frac{\omega_s^3(\omega_p^2 - \gamma^2) - \omega_s \omega_p^4}{(\omega_s^2 - \omega_p^2)^2 + \omega_s^2 \gamma^2} + i \frac{\omega_s^4 \gamma}{(\omega_s^2 - \omega_p^2)^2 + \omega_s^2 \gamma^2} \right] \quad (1)$$

where Δf (Hz) is the shift in QCM-D resonance frequency, ΔD is the change in dissipation, f_F is the fundamental resonance frequency of the sensor (5 MHz), f_s is the QCM-D sensor surface resonance frequency, m_p is the particle mass (kg), ω_s is the sensor resonance angular frequency ($\omega_s = 2 \pi f_s$), ω_p is the particle resonance angular frequency ($\omega_p = 2 \pi f_p$), Z_q is the acoustic impedance of an AT-cut quartz crystal (8.8×10^6 kg m^{-2} s^{-1}), N_p is the number of adhering particles per unit sensor area (m^2), γ equals ξ/m_p with ξ being the drag coefficient (see Fig. 1a), indicative of the viscous component of the bond. The elastic component of the bond follows from ω_p equaling with $\sqrt{k/m_p}$. Note that the coupled resonator model as described in Eq. (1) assumes complete coupling of adhering particles with the sensor surface, including torsion and shear deformation of the sensor surface due to particle oscillations [23]. Moreover, it is assumed that the spring and dashpot are independent from the frequency according to the coupled resonance model, which means that the frequency should not be causing any perturbations of the adhesive bond. Still it should be noted that bond stiffnesses determined using the QCM-D may be influenced by the experimental condition of having been determined in the MHz range.

In this protocol paper, we explain the use the QCM-D and data analysis to obtain elasticities (the spring constant, k) and viscosities (the drag coefficient, ξ) of the bond of biotic and abiotic particles adhering to sensor surfaces, as calculated with the coupled resonator model. Knowledge of the elasticity and viscosity of the bond through which colloidal particles adhere to substratum surfaces will assist in a better understanding of the mechanisms of particle adhesion and in developing new strategies to detach adhering particles from or retaining them on a surface.

2. Materials and preparatory procedures applied

Reagents used

- 1-octadecanothiol (Sigma-Aldrich, Zwijndrecht, The Netherlands)
- 11-mercapto-1-undecanol (Sigma- Aldrich, Zwijndrecht, The Netherlands)
- Ammonia (NH$_3$) (Merck, Darmstadt, Germany)
- Calcium chloride (CaCl$_2$) (Merck, Darmstadt, Germany)
- Ethanol 100% (VWR Chemicals, Fontenay-Sous-Bois, France)
- Hydrogen peroxide (H$_2$O$_2$) (Merck, Darmstadt, Germany)
- Ultrapure water (>18 MΩ cm)
- Potassium chloride (KCl) (Sigma-Aldrich, Zwijndrecht, The Netherlands)
- Potassium phosphate (KH$_2$PO$_4$) (Merck, Darmstadt, Germany)
- Sodium dodecyl sulphate (SDS) 2% (w/v) (Merck, Darmstadt, Germany)
- Silica particles (radius 0.5 μm) (Bangs laboratories, Inc., Fischer, IN, USA)
- Todd Hewitt broth (THB) (Oxoid, Basingstoke, UK).

Main equipment used

- Centrifuge (J-lite, JLA 16.250 Fixed Angle Rotor, Beckman Coulter, CA, USA)
- Sonicator bath (Transsonic TP 640, Elma GmbH & Co Singen, Germany)
- Sonicator (Vibra Cell model 375: Sonica and materials, Danbury CT, USA)
- UV/Ozone (Bioforce Nanosciences, Slough Berkshire, United Kingdom)
- Quartz Crystal Microbalance with Dissipation Monitoring (QCM-D) E1 system (Q-Sense AB, Stockholm, Sweden)
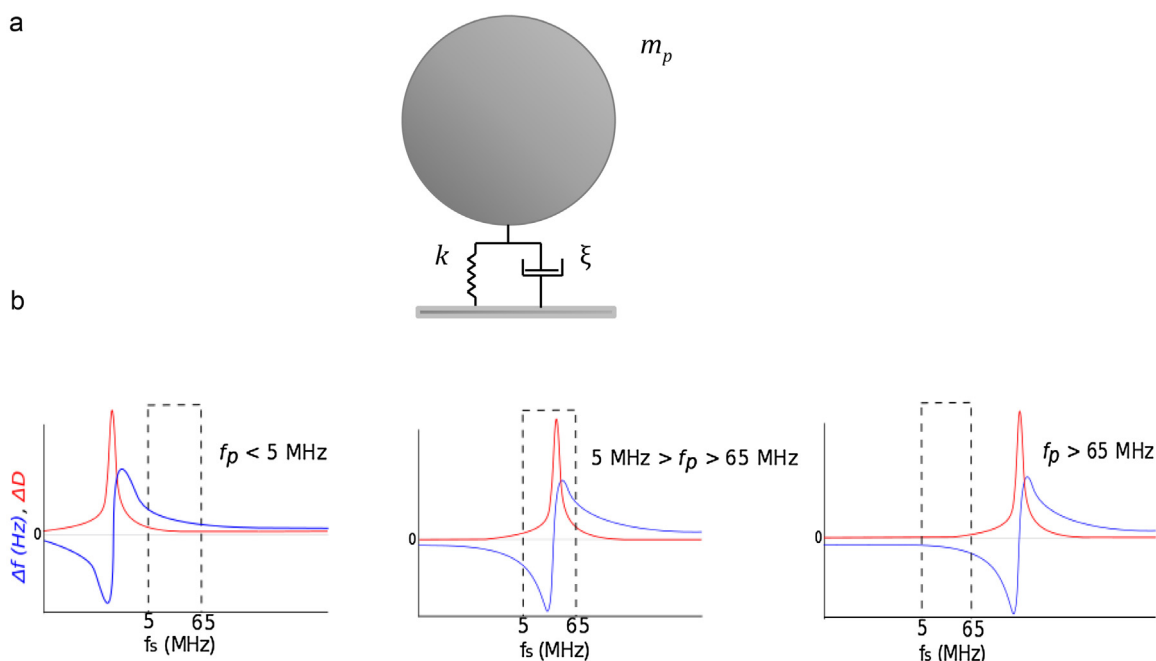
Fig. 1. Schematic diagram of the coupled resonator model.
(a) Colloidal particle with mass, mp adhering to a sensor surface through a viscoelastic bond comprised of a spring with spring constant (k), and dashpot with a drag coefficient (ξ), yielding a particle resonance frequency fp. In the current scheme, spring and dashpot are placed in parallel, *i.e.* as in the Kelvin-Voigt model of viscoelastic response.
(b) Theoretical shifts in the sensor resonance frequency (Δfs) and dissipation changes (ΔD) for particles adhering with different adhesive bond stiffnesses to a QCM-D sensor, as explained in the coupled resonator model, as a function of the QCM-D resonance frequency fs. Particle resonance frequency fp increases with adhesive bond stiffness, and the frequency of zero-crossing (fs = fp) can only be observed within what is referred to as 'the window of observable QCM-D frequencies', including its resonance frequency and overtones, indicated by the dashed rectangles. The asymptotic shift from a negative to a positive Δf occurs when fp equals fs and is accompanied by a maximum in ΔD.

- CCD camera (Model A101, Basler vision technologies, Ahrensburg, Germany)
- Metallurgical microscope with 20x objective (Leica DM2500M, Rijswijk, The Netherlands)
- Peristaltic Pump (Ismatec, Wertheim, Germany)
- QCM crystals with silicon oxide and gold coatings (Q-Sense AB, Stockholm, Sweden).

NOTE Most QCM-D systems operate at a fixed driving power to bring the crystal into resonance. Currently the impact of driving power on the oscillatory behavior of particles adhering to a QCM-D crystal surface is not known.

2.1. Preparatory procedures applied

Preparation of bacterial suspensions. Two days prior to the actual adhesion experiment, make a pre-culture of the bacterial strain, select a single colony from an agar plate and inoculate into 10 ml THB, and incubate at 37 °C. Twenty four hours later, pour the 10 ml solution of THB and bacteria into a 200 ml solution of THB, and grow at 37 °C for 16 h, after which harvesting of the bacteria can begin.

Harvest the bacteria by centrifuging (5 min at 5000g) and by washing the suspension in 100 ml buffer (50 mM potassium chloride, 2 mM potassium phosphate and 1 mM calcium chloride, pH 6.8) two times, followed by sonicating 10 ml of bacterial suspension three times for 10 s at 30 W, while cooling in an ice bath. Sonication is particularly needed for streptococci as they grow in chains, considering single bacteria are preferred for most experiments. Afterwards, the bacterial suspension is centrifuged, and washed one last time in 100 ml buffer before being diluted in the buffer to a final concentration of 3×10^8 bacteria per ml.

Crucial step By washing the bacteria after sonication, it is ensured that free molecules that might have been released during the sonication are removed from the suspension. Free molecules

yield direct mass coupling when adsorbing to a quartz crystal, giving rise to negative frequency shifts during particulate QCM-D measurements, thereby severely complicating data analysis.

Preparation of silica particle suspensions. Silica particles with a radius of 0.5 μm were washed twice by centrifugation in 10 ml of ultrapure water, and diluted to a final concentration of 2×10^8 particles per ml. For the silica particle adhesion experiment, a suspension in 50 mM KCl, pH 6.8 was prepared.

Set-up of the QCM-D. Colloidal particle adhesion is studied under flow using a Q-sense E1 window chamber. For optical monitoring, a CCD camera is connected to the microscope in order to facilitate real-time monitoring of particle adhesion and their enumeration (see Fig. 2). The QCM-D window chamber is disc-shaped (diameter 14 mm) encompassing a volume of approximately 100 μl combined with an inlet and outlet area. Fluid flow is established using a peristaltic pump and can be switched from buffer to a colloidal particle suspension by inserting the attached tubings into a container with the desired fluid.

3. Methods according to protocol

3.1 QCM-D measurement procedure

1. Clean the quartz crystals based on supplier's instructions. Gold coated crystals are generally cleaned by immersion in a 3:1:1 mixture of ultrapure water, NH_3 (28%) and H_2O_2 (30%) at 70 °C for 10 min. Silica coated crystals must be cleaned by submerging them into 2% (w/v) sodium dodecyl sulphate (SDS) for 15 min in a sonicating bath, followed by submersion in ultrapure water also in a sonicating bath for 15 min. As a final step, independent of a possible surface coating of the crystals, it is essential to remove molecular contaminants from the crystal surface by putting them in an UV/ozone environment for 15 min.

Crucial step H_2O_2 should not be added until the temperature of ultrapure water and NH_3 reaches 70 °C as the reaction between
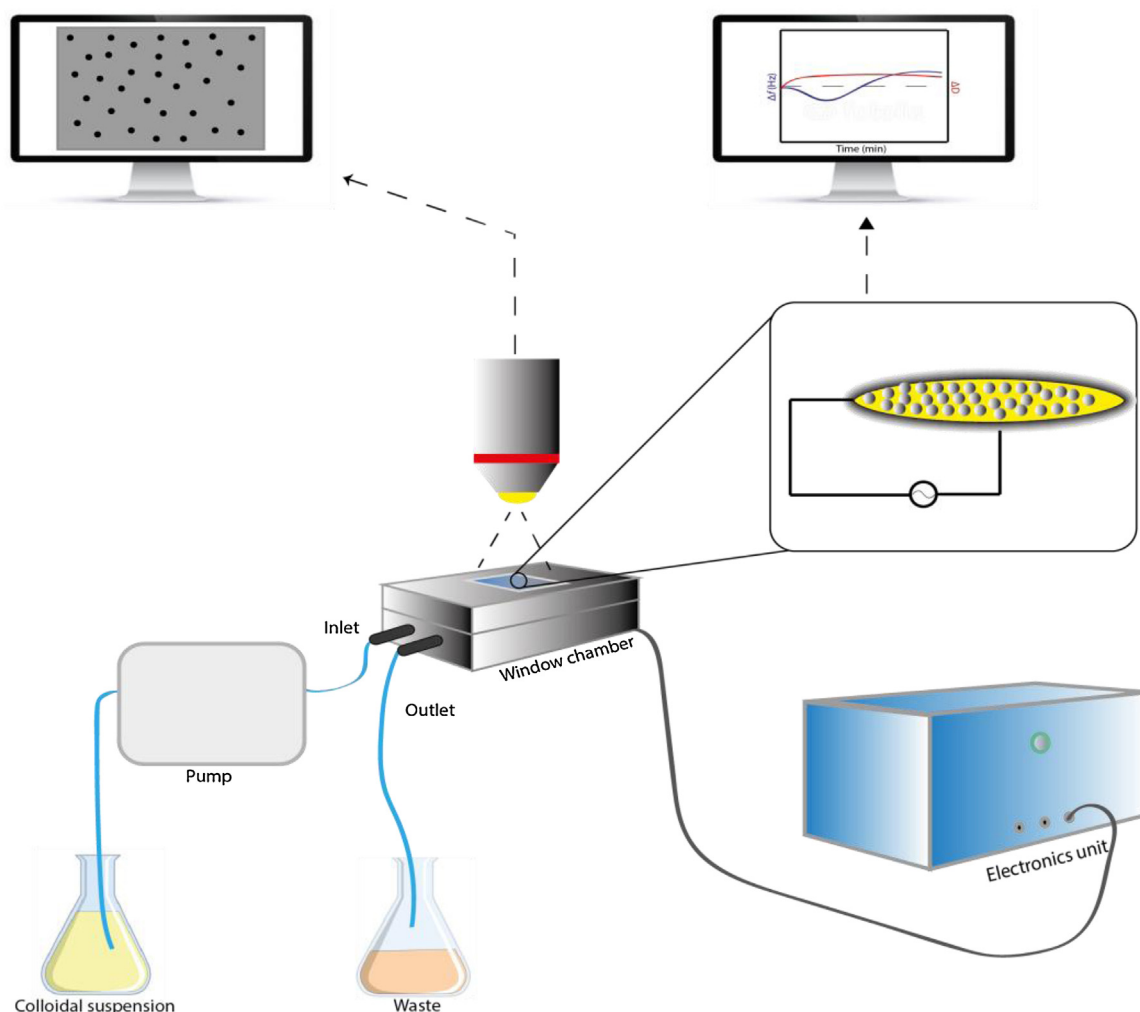
Fig. 2. Schematics of the QCM-D set-up. The set-up consists of an inlet and an outlet where tubings can be attached to leading different fluids through a peristaltic pump through the window chamber into a waste container. In the window chamber, a quartz crystal sensor is placed between a pair of electrodes and by applying an AC voltage over the electrodes, the crystal is brought to oscillation at its acoustic resonance frequency f_s. When this voltage is turned off, the oscillation decays exponentially from which the dissipation can be determined.

NH_3 and H_2O_2 required for proper cleaning of the quartz crystals is less effective at lower temperature.

2. Freshly cleaned gold-coated quartz crystals are hydrophilic by nature, but can simply be made hydrophobic by leaving the cleaned gold crystals overnight in ambient air. The crystal may require a further coating to adjust its surface composition and associated physico-chemical properties. Self-assembled monolayers (SAMs) for instance, can be applied rendering the gold coated crystals hydrophobic by submersing the freshly cleaned crystals into a solution of 0.001 M 1-octadecanethiol or hydrophilic by submersing them into a solution of 0.001 M 11-mercapto-1-undecanol dissolved in 100% ethanol for 18 h.

Crucial step During the coating process, it is important in order to obtain a homogeneous coating on the crystals, that the crystals are left in the solution for the full 18 h, since the alkyl chains need time to align themselves to give a homogeneous coating on the surface. It is advisable to perform some sort of characterization of the crystal surface in order to rule out that possible deviating results are due to aberrant properties of the crystal surface. Water contact angle measurements usually suffice to this end, but when more chemical confirmation of the crystals surface composition is required, X-ray Photoelectron Spectroscopy may be considered, amongst other surface chemical analysis techniques.

3. Mount the cleaned or coated crystal in the QCM-D

Crucial step After mounting of the crystal, it is crucial that the window chamber is not tightened too strongly, since crystals may break due to the excessive pressure.

4. Switch on the QCM-D and controlling software. Adjust the setting to the desired temperature. Throughout this protocol, we have done all our measurements at 21 °C.

5. Close the window chamber and obtain the crystal's resonance frequencies and dissipation values at the fundamental frequency and observable overtones in order to ensure that the crystal is in good condition.

Crucial step The dissipation value at the crystals fundamental frequency should be around 40×10^{-6} or less (oral communication with application specialist, Q-Sense, Biolin Scientific AB Västra Frölunda, Sweden). If the dissipation value deviates more than 5×10^{-6} from this "normal" value, its cause should first be determined before continuing the experiment. Sometimes it helps to loosen or tighten the screws that hold the crystal in the window chamber in order to regain "normal" values. In other cases it may help to take the entire window chamber apart and remount the crystal. If nothing helps, the crystal has to be replaced.

6. Connect the tubings to the QCM-D chamber and start the peristaltic pump to introduce a flow (300 μl/min) of buffer through the QCM-D window chamber.
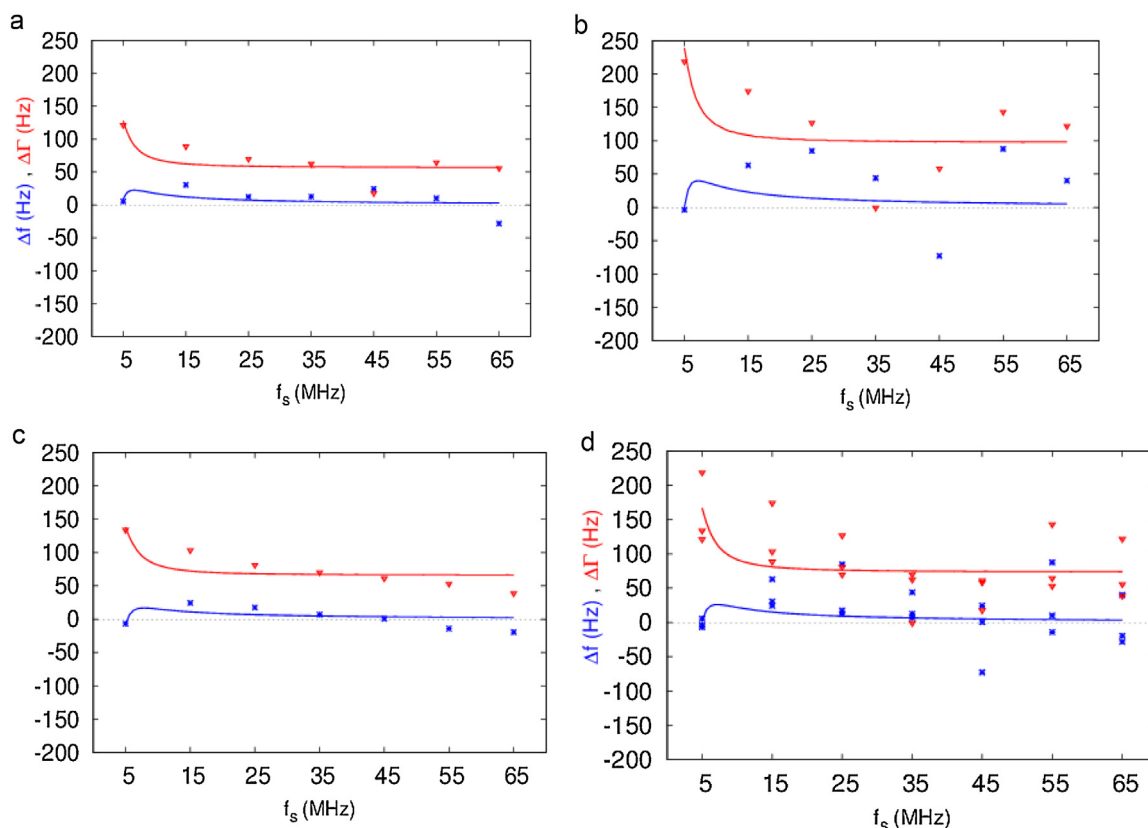
Fig. 3. Comparison of using seven data points of triplicate experiments in separate brute force fits (a–c) *versus* the use of 21 data points in one brute force fit (d) for the derivation of the spring constant k, the drag coefficient ξ and the particle mass m_p from the QCM-D output for *S. salivarius* HB7 adhering on a hydrophobic SAM on the crystal sensor surface. Note that in previous studies QCM-D data and fitting were presented in so-called polar plots of Δf *versus* $\Delta \Gamma$ [27], we prefer to present both Δf and $\Delta \Gamma$ *versus* f as two separate functions, the blue line representing Δf and the red line representing $\Delta \Gamma$ as a function of the sensor resonance frequency. (For interpretation of the references to colour in this figure legend, the reader is referred to the web version of this article.)
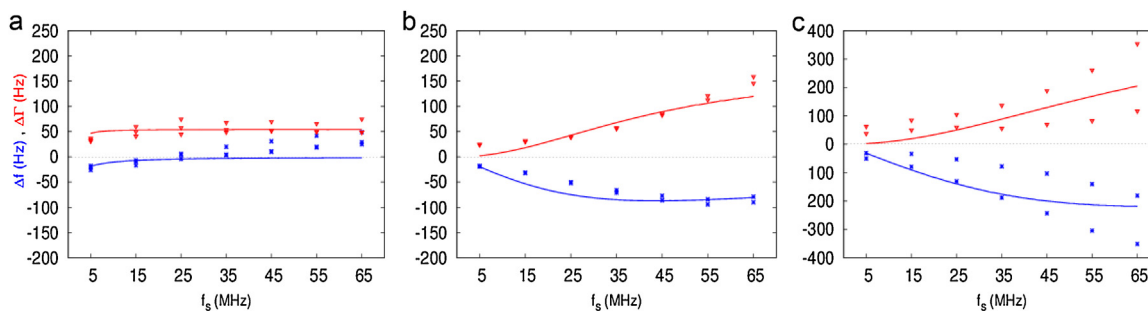

Fig. 4. Δf (blue) and $\Delta \Gamma$ (red) *versus* f_s for abiotic silica particles and silica particles coated with streptavidin, adhering to a silica sensor crystal or a silica sensor coated with a biotinylated PEG alkane thiol. (For interpretation of the references to colour in this figure legend, the reader is referred to the web version of this article.)
(A) silica particles on a silica crystal.
(B) silica particles on a biotinylated PEG alkane thiol coated silica crystal.
(C) streptavidin coated silica particles on biotinylated PEG alkane thiol coated silica crystal.

Crucial step It is crucial to ensure that filling of the system is done free of air bubbles. Air bubbles can be prevented by tilting the window chamber during filling with buffer, thereby allowing the buffer to slowly run into the chamber and displace all air. In case air bubbles are formed, they can often be removed by increasing the speed of the fluid flow to force the bubbles out of the system. It is also possible to de-aerate the buffers by sonication prior to using them in the experiment. Air bubbles can specifically arise when working with crystals coated with a hydrophobic coating.

7. Find resonance frequencies and dissipation values of the sensor crystal in buffer by letting the buffer flow through the system until the frequency is stabilized, typically requiring approximately 5 min. Stability is accepted when the drift in frequency shifts for all observable overtones is less than 2 Hz per 10 min.

Crucial step It is advised to set up a log-journal of crystal resonance frequencies and dissipation values in buffer as well as in air to define "normal" values in both media for the specific use made. After filling the chamber with buffer, dissipation values usually increase, but this increase should never be more than ten-fold (oral communication with application specialist, Q-Sense, Biolin Scientific AB Västra Frölunda, Sweden). Aberrant resonance frequencies and dissipation values after filling the chamber with buffer can be due to the presence of minor air bubbles in the chamber.

Table 1

Values for the spring constant k, drag coefficient ξ and mass of the particles m_p obtained using seven data points of triplicate experiments in separate brute force fits (see also Fig. 3a–c) *versus* the use of 21 data points in one brute force fit (see Fig. 3d) in a Kelvin-Voigt model. RMSD indicates the quality of the brute force fit.

S. salivarius HB7 on a hydrophobic SAM	k (kg/s^2)	ξ (10^{-9} kg/s)	m_p (10^{-16} kg)	RMSD (Hz)
Experiment 1, seven data points	0.24	6	5	23
Experiment 2, seven data points	0.48	12	8	72
Experiment 3, seven data points	0.35	11	6	20
Averaged of experiment 1–3 output parameters	0.36 ± 0.12	10 ± 3	6 ± 2	–
Experiments 1–3 containing 21 data points	0.36	10	7	42

8. Introduce the suspension containing either biotic or abiotic particles, typically at particle concentrations of around 10^8 particles per ml. Particle adhesion proceeds at a speed that mainly depends on their sedimentation in suspension and is usually faster for particles with a higher specific density. A surface density of 10^{10} particles adhering per m^2 should be aimed for, yielding a surface coverage for micron-sized colloidal particles that prevents them from touching each other. Particle adhesion should be monitored using the microscope mounted CCD camera. Following the appropriate adhesion time, the number of adhering particles must be determined using image analysis software, which can be easily written using the Matlab platform. Appropriate programs for biological analysis can also be downloaded for free from the internet, such as ImageJ, CellProfiler and Fiji [24].

Crucial step In order to count the number of adhering colloidal particles properly using the CCD camera, it is important that buffer is running through the system in order to remove any non-adhering particles from the chamber and prevent them from intervening with the enumeration of adhering ones. Alternatively for kinetic analysis of particle adhesion during flow with a particle suspension, image analysis software that filters out particles that change position along with the fluid flow should be used [25].

9. The frequency shifts and dissipation changes are retrieved from the QCM-D at the crystals fundamental frequency and its overtones, and are subsequently used in Eq. (1). For the purpose of later fitting it is advantageous to convert dissipation changes (ΔD) into $\Delta\Gamma$ values ((ΔDf_s)/2), that is the half bandwidth at half height ("bandwidth") of the resonance curve [26]. These data are then used to fit the parameters occurring in Eq. (1) using a brute force fitting program in Fortran 90 (see Supplementary material) to derive values for the spring constant k the drag coefficient, ξ, the particle mass m_p, and the quality of the fit or the Root Mean Squared Deviation (RMSD).

Crucial step The number of data points that can be obtained per experiment is restricted by the number of overtones that can be observed. With the instrument used in our studies, a maximum of seven data points for Δf and $\Delta\Gamma$ as a function of the crystals resonance frequency can be obtained in each experiment. This is not necessarily enough to reliably calculate all output parameters since the iterative numerical procedure can easily get trapped in local minima yielding physically unrealistic results, most noticeably for the particle mass and output data should be critically evaluated for being physically realistic. For validation of the output, we suggest to

compare the mass derived from the QCM-D output with the particle mass calculated from its dimensions and specific density.

3.2. Analysis of brute force fitting of QCM-D output to a coupled resonator model

Given that only seven values of Δf and ΔD are available and that, also, the scatter in the data is frequently considerable, it is essential to devise a fitting algorithm, which is robust to avoid physically unrealistic results. A brute force algorithm is a generic problem-solving algorithm in which all possible data points are employed to obtain the best fitting parameters, while checking whether each fit satisfies the problem's statement. By implementing this brute force technique, physically unrealistic, erroneous output is prevented due to solutions getting trapped in local minima of the fitting algorithm. The algorithm achieves robustness by defining the lower and upper bound of the three output parameters *i.e.* m_p, k and ξ and then the algorithm defines a grid of choices for parameters (typically $100 \times 100 \times 100$ parameter combinations) and searches the global minimum of the root-mean-squared deviation between the data and the fit. Care should be taken however, that fitted parameters do not hit the boundaries installed and whenever this is the case, boundaries should be widened.

To demonstrate advantages and disadvantages of using seven data points of, for instance, triplicate experiments in separate brute force fits *versus* the use of all 21 data points in one brute force fit for the derivation of the spring constant k, the drag coefficient ξ and the particle mass m_p from the QCM-D output, we firstly present results from triplicate experiments with separate bacterial cultures each comprising seven data points. In the specific example chosen (see Fig. 3a–c and Table 1) we aimed to analyze the properties of the bond between a streptococcal bacterium, *Streptococcus salivarius* HB7 possessing 91 nm long fibrillar surface appendages, and a hydrophobic SAM on the crystal sensor surface. Results of fitting the three parameters occurring in Eq. (1) to the data points in each of the three experiments can be seen in Fig. 3a–c, while resulting output parameters including the root mean square deviation (RMSD) values describing the quality of the fits are presented in Table 1. On average, physically realistic results are obtained with the average particle mass (the only output parameter that can be compared with an expected value as can be found in the literature) coinciding well with the one based on particle dimensions and specific density (5×10^{-16} kg). Qualities of the fit are variable across the three

Table 2

Spring constants k, drag coefficients ξ and masses of abiotic and biotic particles, m_p, adhering to various crystal surfaces, including the RMSD indicating the quality of the brute force fit to the QCM-D output.

	k (kg/s^2)	ξ (10^{-9} kg s^{-1})	m_p (10^{-16} kg)	RMSD (Hz)
Abiotic particles: silica particles				
Silica particles-silica crystal surface	0	16	13	18
Silica particles-biotinylated crystal surface	0	102	4	18
Streptavidin coated particles-biotinylated crystal surface	0.08	279	6	78
Biotic particles: S. salivarius HB7				
On a hydrophobic Au surface	0.21	10	7	19
On a hydrophobic SAM	0.35	10	6	42
On a hydrophilic SAM	0.23	5	5	89

experiments though. Next, all 21 data points were subjected to a single brute force analysis (see Fig. 3d and Table 1), yielding nearly identical results for the spring constant, drag coefficient and particle mass as obtained after averaging the three data sets comprising seven data points. Thus there are no overriding arguments to either use seven data points from multiple experiments in separate brute force fits *versus* the use of all data combined in one brute force fit, else than that fitting 21 points directly yields an RMSD value, opposite to averaging three individual fits.

The assumption underlying Eq. (1) that all adhering particles couple completely with the sensor surface to cause torsion and shear deformation is not necessarily true, which reflects in minor deviations of the particle mass derived from the true particle mass [23]. Another assumption underlying Eq. (1) is that all adhering particles possess identical size and shape. Polydispersity however, may give rise to a distribution in angular particle frequency [20,23], that can be accounted for by adding a polydispersity parameter to Eq. (1). Although this may increase the quality of the fit, and possibly avoid overly small spring constants as observed for silica particles on silica crystal surfaces and biotinylated crystal surfaces (see Table 2), fitting of four parameters to a complicated equation as Eq. (1) with only a limited number of discrete data point bears the risk of yielding physically unrealistic values.

4. Duration of experiment

In this estimate of the time required for experiments, we neglect the time to prepare particle suspensions, as preparation of biotic particle suspensions usually requires much more time due to culturing than abiotic particles suspensions, especially when commercially purchased. Once a particle suspension has been prepared, a typical QCM-D experiment as described above, should not take more than 4 h to perform. Brute force fitting of the data can be done within 30 min after measurements.

5. Expected results

All quantitative properties of the adhesive bond reported in this section have been obtained by fitting k, ξ, and m_p, as occurring in Eq. (1) to the QCM-D frequency shifts and dissipation changes at the observable frequencies using a brute force fitting algorithm and using all data points available in a single fit without averaging data obtained in separate experiments at the same frequency. Fig. 4 depicts the fit to Eq. (1) of experimental data for abiotic silica particles and silica particles coated with streptavidin, adhering to a silica sensor crystal or a silica sensor coated with biotinylated polyethylene glycol (PEG) alkane thiol. Visual inspection of the graphs shows a good fit to the data points.

Good quality of the fit is confirmed by the relatively low RMSD values of the fits summarized in Table 2, with the exception of the fit for the experiments comprising streptavidin coated silica particles on biotinylated PEG alkane thiol coated silica crystal. Values for k and ξ reflect the influence of an adsorbed protein film on the crystal surface *versus* a bare crystal surface on the adhesive bond properties (higher drag coefficient) as well as the impact of specific ligand-receptor binding *versus* non-specific binding (higher spring constants and drag coefficients). Importantly, although values for the particle mass m_p obtained vary over a factor of three (see also Table 2), they are of the same order of magnitude as expected for 1 μm diameter silica particles (14×10^{-16} kg).

Table 2 also illustrates the anticipated results for the adhesion of *S. salivarius* HB7 adhering to different crystal surfaces. Most noticeably, spring constants k of the streptococcal bond are higher than for abiotic silica particles with little influence of the crystal surface properties. The drag coefficient ξ however, is orders of magnitude smaller than for abiotic silica particles, indicating that lower friction losses due to oscillations as a result of the lower weight and density of the biotic particles. Note that in all cases, the bacterial mass m_p obtained in the fit matches very well with the mass expected for bacteria (5×10^{-16} kg).

In summary, the proposed protocol involves the use of a coupled resonator model to obtain values for the spring constant and drag coefficient of the bond between adhering biotic and abiotic particles on QCM-D crystal surfaces as well as their masses. These three output parameters are fitted to the QCM-D output Δf and $\Delta \Gamma$ as a function of the crystals resonance frequencies within the window of observable frequencies. Knowledge of the bond properties in particular adhesion to a solid-liquid interface allows better understanding on how to influence particle adhesion and detachment.

6. Future prospects

QCM-D data analysis for particle adhesion is neither trivial nor beyond dispute. Other viscoelastic models than the Kelvin-Voigt model implemented in Eq. (1), such as the Maxwell model (spring and dashpot placed in series) might improve the quality of the fit and yield lower RMSD values (D. Johannsmann, private communication). As most "one-by-one" methods to derive viscoelastic bond properties indicate large standard deviations over individual particles, inclusion of a polydispersity parameter in Eq. (1) is also worthwhile to attempt in order to improve the quality of fitting. Finally, as molecular adsorption of bacterial bi-products such as polysaccharides, proteins and DNA is hard to avoid, analyses of combined molecular adsorption and resonator coupling by introducing an offset in frequency and dissipation in Eq. (1) to differentiate between molecular adsorption and mass-coupling might increase the ease of use of QCM-D preparatory steps for bacterial adhesion studies.

Competing interests

HJB is also director of a consulting company, SASA BV (GN Schutterlaan 4, 9797 PC Thesinge, The Netherlands). The authors declare no potential conflicts of interest with respect to authorship and/or publication of this article. Opinions and assertions contained herein are those of the authors and are not construed as necessarily representing views of their respective employers.

Acknowledgements

Appendix A. Supplementary data

Supplementary data associated with this article can be found, in the online version, at http://dx.doi.org/10.1016/j.colsurfb.2016.08.062.

References

[1] R.O. Darouiche, Device-associated infections: a macroproblem that starts with microadherence, Clin. Infect. Dis. 33 (2001) 1567–1572.
[2] B. Serra, M. Gamella, A.J. Reviejo, J.M. Pingarrón, Lectin-modified piezoelectric biosensors for bacteria recognition and quantification, Anal. Bioanal. Chem. 391 (2008) 1853–1860.
[3] R.C. Hayward, D.A. Saville, I.A. Aksay, Electrophoretic assembly of colloidal crystals with optically tunable micropatterns, Nature 404 (2000) 56–59.
[4] A. Pomorska, D. Shchukin, R. Hammond, M.A. Cooper, G. Grundmeier, D. Johannsmann, Positive frequency shifts observed upon adsorbing micron-sized solid objects to a quartz crystal microbalance from the liquid phase, Anal. Chem. 82 (2010) 2237–2242.

[5] D. Johannsmann, Viscoelastic analysis of organic thin films on quartz resonators, Macromol. Chem. Phys. 516 (1999) 501–516.

[6] B.W. Peterson, Y. He, Y. Ren, A. Zerdoum, M.R. Libera, P.K. Sharma, et al., Viscoelasticity of biofilms and their recalcitrance to mechanical and chemical challenges, FEMS Microbiol. Rev. 39 (2015) 234–245.

[7] T. Dabros, P. Warszynski, T.G.M. van de Ven, Motion of latex spheres tethered to a surface, J. Colloid Interface Sci. 162 (1994) 254–256.

[8] P. Stoodley, Z. Lewandowski, J.D. Boyle, H.M. Lappin-Scott, Structural deformation of bacterial biofilms caused by short-term fluctuations in fluid shear: an in situ investigation of biofilm rheology, Biotechnol. Bioeng. 65 (1999) 83–92.

[9] Y.F. Dufrêne, Towards nanomicrobiology using atomic force microscopy, Nat. Rev. Microbiol. 6 (2008) 674–680.

[10] D.J. Muller, AFM: a nanotool in membrane biology, Biochemistry 47 (2008) 7986–7998.

[11] C.J. Wright, I. Armstrong, The application of atomic force microscopy force measurements to the characterisation of microbial surfaces, Surf. Interface Anal. 38 (2006) 1419–1428.

[12] K.C. Neuman, A. Nagy, Single-molecule force spectroscopy: optical tweezers, magnetic tweezers and atomic force microscopy, Nat. Methods 5 (2008) 491–505.

[13] S. Lu, G. Walters, R. Parg, J.R. Dutcher, Nanomechanical response of bacterial cells to cationic antimicrobial peptides, Soft Matter 10 (2014) 1806–1815.

[14] Y. Chen, W. Norde, H.C. van der Mei, H.J. Busscher, Bacterial cell surface deformation under external loading, MBio 3 (2012) 1–7.

[15] L. Song, J. Sjollema, P.K. Sharma, H.J. Kaper, H.C. van der Mei, H.J. Busscher, Nanoscopic vibrations of bacteria with different cell-wall properties adhering to surfaces under flow and static conditions, ACS Nano 8 (2014) 8457–8467.

[16] M. Kamiti, T.G.M. Van De Ven, Measurement of spring constants of polyacrylamide chains bridging particles to a solid surface, Macromolecules 29 (1996) 1191–1194.

[17] G. Sauerbrey, Verwendung von Schwingquarzen zur Wägung dünner Schichten und zur Mikrowägung, Zeitschrift Für Phys. 155 (1959) 206–222.

[18] J.N. D'Amour, J.J.R. Stålgren, K.K. Kanazawa, C.W. Frank, M. Rodahl, D. Johannsmann, Capillary aging of the contacts between glass spheres and a quartz resonator surface, Phys. Rev. Lett. 96 (2006).

[19] G.L. Dybwad, A sensitive new method for the determination of adhesive bonding between a particle and a substrate, J. Appl. Phys. 58 (1985) 2789–2790.

[20] A.L.J. Olsson, H.C. van der Mei, D. Johannsmann, H.J. Busscher, P.K. Sharma, Probing colloid-substratum contact stiffness by acoustic sensing in a liquid phase, Anal. Chem. 84 (2012) 4504–4512.

[21] D. Johannsmann, Viscoelastic mechanical, and dielectric measurements on complex samples with the quartz crystal microbalance, Phys. Chem. Chem. Phys. 10 (2008) 4516–4534.

[22] V. Vadillo-Rodriguez, S.R. Schooling, J.R. Dutcher, In situ characterization of differences in the viscoelastic response of individual gram-negative and gram-positive bacterial cells, J. Bacteriol. 191 (2009) 5518–5525.

[23] A. Peschel, A. Langhoff, D. Johannsmann, Coupled resonances allow studying the aging of adhesive contacts between a QCM surface and single, micrometer-sized particles, Nanotechnology 26 (2015) 484001.

[24] K.W. Eliceiri, M.R. Berthold, I.G. Goldberg, L. Ibáñez, B.S. Manjunath, M.E. Martone, et al., Biological imaging software tools, Nat. Methods 9 (2012) 697–710.

[25] J.M. Meinders, H.C. van der Mei, H.J. Busscher, Deposition efficiency and reversibility of bacterial adhesion under flow, J. Colloid Interface Sci. 176 (1995) 329–341.

[26] I. Reviakine, D. Johannsmann, R.P. Richter, Hearing what you cannot see and visualizing what you hear, Anal. Chem. 83 (2011) 8838–8848.

[27] A.L.J. Olsson, N. Arun, J.S. Kanger, H.J. Busscher, I.E. Ivanov, T.A. Camesano, et al., The influence of ionic strength on the adhesive bond stiffness of oral streptococci possessing different surface appendages as probed using AFM and QCM-D, Soft Matter 8 (2012) 9870.

Quantification of the Viscoelasticity of the Bond of Biotic and Abiotic Particles Adhering to Solid-Liquid Interfaces Using a Window-equipped Quartz Crystal Microbalance with Dissipation

Rebecca van der Westen, Henny C. van der Mei, Hans De Raedt, Adam L. J. Olsson, Henk J. Busscher & Prashant K. Sharma

Supplementary Material

FORTRAN 90 code for brute force fitting of QCM-D output to Equation 1 and obtain the m_p, k and ξ parameters

```fortran
!=========================================================================
!
! Brute force fitting to damped harmonic oscillator model
!
!=========================================================================

implicit real(kind=8) (a-h,o-z)
parameter (maxitems=100)
character(len=1024) :: line,f1,f2,word
real(kind=8),dimension(0:100):: frplot,fiplot ! real and imaginary part for plotting
real(kind=8),dimension(maxitems):: f,fr,fi ! frequecies, real and imaginary part of data
logical :: exists
CALL GET_COMMAND(line) ! get command line and strip command itself
line=adjustl(line)
i=index(trim(line)," ")
if(i>0) then
line=line(i+1:)
else if(len_trim(line)>0) then
line=" "
endif
read(line,*,iostat=ios) f1,item1,item2,iterations ! read the data on the command line
if(ios/=0.or.item1<=0.or.item2<item1) then ! in case iterations is not specified, use default
iterations=12
read(line,*,iostat=ios) f1,item1,item2
if(ios/=0.or.item1<=0.or.item2<item1) then ! in case item1 and item2 are not specified, use
defaults
item1=1
item2=maxitems
read(line,*,iostat=ios) f1 ! read the input file name
if(ios/=0) then
f1="S.aureus on Hydrophobic gold" ! default input file name
endif
endif
endif
! check input files etc.
i=index(trim(f1),".dat",.True.)
if(i>0) f1=trim(f1(1:i-1)) ! strip .dat extension if present
inquire(file=trim(f1)//".dat",exist=exists) ! data should be in f1.dat
if(.not.exists) then
write(6,'(1x,"Where is data file ",a," ?")') trim(f1)//".dat"
stop
endif
f2=trim(f1)//".parameters" ! check if f1.parameters.dat
exists=.false.
```

```fortran
inquire(file=trim(f2)//".dat",exist=exists)
if(.not.exists) then ! if not, write a f1.parameters.dat for later use
write(6,'(1x,"Could not find parameter file ",a)') trim(f2)//".dat"
write(6,'(1x,"Creating parameter file ",a," using defaults")') trim(f2)//".dat"
open(unit=1,file=trim(f2)//".dat",status="new")
write(1,'(" Na Amin Amax, Nf fmin fmax, NG Gmin Gmax")')
Na=200 ! # points in A-space
Amin=1 ! A is searched in [Amin,Amax]
Amax=100
Nb=200 ! # points in f-space
fmin=0 ! f is searched in [fmin,fmax]
fmax=100
Nc=200 ! # points in G-space
Gmin=1 ! G is searched in [Gmin,Gmax]
Gmax=100
write(1,'(3(i5,2f10.1))') Na,Amin,Amax,Nb,fmin,fmax,Nc,Gmin,Gmax
close(1)
else ! if the f1.parameters.dat exists, use the values in this file
open(unit=1,file=trim(f2)//".dat",status="old")
write(6,'(1x,"Reading parameter file: ",a)') trim(f2)
read(1,*,iostat=ios) word
if(ios/=0) stop "There is something wrong with the parameter file"
read(1,*,iostat=ios) Na,Amin,Amax,Nb,fmin,fmax,Nc,Gmin,Gmax
if(ios/=0) stop "There is something wrong with the parameter file"
close(1)
Na=max(10,Na)
r0=Amin
r1=Amax
Amin=max(min(r0,r1),0.)
Amax=max(r0,r1)
Nb=max(10,Nb)
r0=fmin
r1=fmax
fmin=max(min(r0,r1),0.)
fmax=max(r0,r1)
Nc=max(10,Nc)
r0=Gmin
r1=Gmax
Gmin=max(min(r0,r1),0.)
Gmax=max(r0,r1)
write(6,'(1x," Na Amin Amax, Nf fmin fmax, NG Gmin Gmax")')
write(6,'(1x,3(i5,2f10.1))') Na,Amin,Amax,Nb,fmin,fmax,Nc,Gmin,Gmax
endif
write(6,'(1x,"Reading data file: ",a)') trim(f1)//".dat" ! read all items from data file f1.d
at
open(unit=1,file=trim(f1)//".dat",status="old")
items=0
ios=0
do while (ios==0)
read(1,'(a)',iostat=ios) line
if(ios/=0) cycle
read(line,*,iostat=ios0) xxx,x,y,z
if(ios0/=0) cycle
items=items+1
if(items>maxitems) stop 'items>maxitems ?'
f(items)=x
fr(items)=y
fi(items)=z
enddo
close(1)
write(6,*) "read ",items," lines"
item2=min(items,item2)
```

```fortran
j=0
do i=item1,item2 ! select items from item1 to item2
j=j+1
f(j)=f(i)
fr(j)=fr(i)
fi(j)=fi(i)
enddo
items=j
write(6,*) "working with lines ",item1," to ",item2
if(item2>items) item2=items
write(word,'(a,"_",i0,"_",i0)') trim(f1),item1,item2 ! file name contains the range of items
selected
open(unit=1,file=trim(word)//".plot",status="unknown") ! create a file with (selected) data t
o be used for plottimg
do j=1,items
write(1,'(i4,3f15.3)') j,f(j),fr(j),fi(j)
enddo
close(1)
r0=items
r0=sqrt(r0/(r0-3))
call Search(f,fr,fi,items,Amin,Amax,Na,fmin,fmax,Nb,Gmin,Gmax,Nc, Asol,Bsol,Csol,smin)
write(6,'(1x," Na Amin Amax, Nf fmin fmax, NG Gmin Gmax")')
write(6,'(1x,3(i5,2f10.1))') Na,Amin,Amax,Nb,fmin,fmax,Nc,Gmin,Gmax
write(6,'(1x," A = ",f0.2,", omega_p = ",f0.2,", Gamma = ",f0.2,", RMS = ",f0.3,", data point
s = ",i0)') Asol,Bsol,Csol,smin*r0,items
write(6,*)
fac=0.1
do i=1,3*(iterations/3) ! loop to reduce the search box
smin0=smin
a0=amin
a1=amax
b0=fmin
b1=fmax
c0=Gmin
c1=Gmax
call random_number(r1)
r1=(1-2*fac)*r1+fac
select case (mod(i-1,3))
case (0) ! change A
if(Asol-Amin<Amax-Asol) then
amax=Asol+(Amax-Asol)*r1
else
amin=Asol+(Amin-ASol)*r1
endif
case (1) ! change f
if(Bsol-fmin<fmax-Bsol) then
fmax=Bsol+(fmax-Bsol)*r1
else
fmin=Bsol+(fmin-Bsol)*r1
endif
case (2) ! change G
if(Csol-Gmin<Gmax-Csol) then
Gmax=Csol+(Gmax-Csol)*r1
else
Gmin=Csol+(Gmin-Csol)*r1
endif
end select
call Search(f,fr,fi,items,Amin,Amax,Na,fmin,fmax,Nb,Gmin,Gmax,Nc, Asol,Bsol,Csol,smin)
if(mod(i-1,3)==2) then ! print some output every now and then
write(6,'(1x," Na Amin Amax, Nf fmin fmax, NG Gmin Gmax")')
write(6,'(1x,3(i5,2f10.1))') Na,Amin,Amax,Nb,fmin,fmax,Nc,Gmin,Gmax
write(6,'(1x," A = ",f0.2,", omega_p = ",f0.2,", Gamma = ",f0.2,", RMS = ",f0.3)') Asol,Bsol,
```

```fortran
      Csol,smin*r0
      write(6,*)
      endif
      if(smin>smin0) then ! if changing the search box was unsuccessful, reset the size
      select case (mod(i-1,3))
      case (0)
      amin=a0
      amax=a1
      case (1)
      fmin=b0
      fmax=b1
      case(2)
      Gmin=c0
      Gmax=c1
      end select
      endif
      enddo ! do i=1,3*(iterations/3) ! loop to try to reduce the search box
      ! print final results
      write(6,'(1x," Na Amin Amax, Nf fmin fmax, NG Gmin Gmax")')
      write(6,'(1x,3(i5,2f10.1))') Na,Amin,Amax,Nb,fmin,fmax,Nc,Gmin,Gmax
      write(6,'(1x," A = ",f0.2,", omega_p = ",f0.2,", Gamma = ",f0.2,", RMS = ",f0.3,", data point
      s = ",i0)') Asol,Bsol,Csol,smin*r0,items
      write(6,*)
      open(unit=2,file=trim(word)//".par",status="unknown") ! write parameters to file for plotting
      purposes
      write(2,'(4f10.2)') Asol,Bsol,Csol,smin*r0
      close(2)
      call Plot(f,items,Asol,Bsol,Csol,frplot,fiplot) ! generate data for plot
      open(unit=2,file=trim(word)//".fit",status="unknown") ! write fitted function for plotting pu
      rposes
      do k=0,100
      write(2,'(3e11.3)') (maxval(f(1:items))*k+minval(f(1:items))*(100-k))/100,frplot(k),fiplot(k)
      enddo
      close(2)
      end


!!!!!!!!!!!!!!!!!!!!!!!!!!!!!!!!!!!!!!!!!!!!!!!!!!!!!!!!!!!!!!!!!!!!!!!!!!!!!!!!!!!!!!!!!!!!!!!!!!!!!!!!
      subroutine Search(f,fr,fi,n, a0,a1,Na, b0,b1,Nb,c0,c1,Nc, amin,bmin,cmin,smin) ! brute-force
      search for minimum RMS
      implicit real(kind=8) (a-h,o-z)
      real(kind=8),dimension(n):: f,fr,fi
      smin=huge(s)
      amin=0
      bmin=0
      cmin=0
      do i=0,Nb
      b=(b1*i+b0*(Nb-i))/Nb
      b2=b*b
      do j=0,Nb
      c=(c1*j+c0*(Nc-j))/Nc
      c2=c*c
      do l=0,Na
      a=(a1*l+a0*(Na-l))/Na
      s=0
      do k=1,n
      x=f(k)
      x2=x*x
      b2x2=b2-x2
      b2x2=a/(b2x2*b2x2+x2*c2)
      rr=b2x2*x*(x2*(b2-c2)-b2*b2)-fr(k) ! rr=a*x*(x*x*(b*b-c*c)-b**4)/((b*b-x*x)**2+x*x*c*c)
      ri=b2x2*x2*x2*c-fi(k) ! ri=a*x**4*c/((b*b-x*x)**2+x*x*c*c)
```

```fortran
        s=s+rr*rr+ri*ri
      enddo
      if(s>smin) cycle
      smin=s
      amin=a
      bmin=b
      cmin=c
    enddo
  enddo
enddo
smin=sqrt(smin/n/2)
end Subroutine
subroutine Plot(f,n,amin,bmin,cmin,frplot,fiplot) ! generate data for plot
implicit real(kind=8) (a-h,o-z)
real(kind=8),dimension(n):: f,fr,fi
real(kind=8),dimension(0:100):: frplot,fiplot
b2=bmin*bmin
c2=cmin*cmin
f0=minval(f)
f1=maxval(f)
do k=0,100
  x=(f1*k+f0*(100-k))/100
  x2=x*x
  b2x2=b2-x2
  b2x2=amin/(b2x2*b2x2+x2*c2)
  frplot(k)=b2x2*x*(x2*(b2-c2)-b2*b2) ! rr=a*x*(x*x*(b*b-c*c)-b**4)/((b*b-x*x)**2+x*x*c*c)
  fiplot(k)=b2x2*x2*x2*cmin ! ri=a*x**4*c/((b*b-x*x)**2+x*x*c*c)
enddo
end Subroutine
```